# The influence of metamorphic grade on arsenic in metasedimentary bedrock aquifers: A case study from Western New England, USA

Peter C. Ryan [a,*], David P. West [a], Keiko Hattori [b], Sarah Studwell [a], David N. Allen [c], Jonathan Kim [d]

[a] Geology Department, Middlebury College, Middlebury, VT 05753, USA
[b] Department of Earth Sciences, University of Ottawa, Ottawa K1N 6N5, Canada
[c] Biology Department, Middlebury College, Middlebury, VT 05753, USA
[d] Vermont Geological Survey, Montpelier, VT 05620-3902, USA

## HIGHLIGHTS

- Variability in As content was examined in a metasedimentary bedrock aquifer system.
- As contents of rock and water are both inversely proportional to metamorphic grade.
- Pyrite recrystallization in upper chlorite zone liberates As into metamorphic fluids.
- The high mobility of As enables it to be leached out of metapelites.

## ARTICLE INFO

## ABSTRACT

Elevated As occurs in many meta-sedimentary bedrock aquifers where elevated bulk-rock As content is one of the primary controls on the concentration of As in groundwater. This study was designed to determine As concentrations in a black shale, black slate and black phyllite sequence that comprises the bedrock aquifer system of the Taconic Mountain region of southwestern Vermont and adjacent New York State. Variability in groundwater As concentrations provides the impetus for this study: 25% of wells in weakly metamorphosed shales and slates (<lower chlorite zone) exceed 10 µg/L (133 nmol/L) As, yet only 3% of wells in stratigraphically-equivalent phyllites (metamorphosed to ≥upper chlorite zone) exceed 10 µg/L As. Geochemical analysis indicates that whole-rock As content is inversely proportional to metamorphic grade, ranging from a mean of 26.9 mg kg$^{-1}$ in low-grade black shales and slates to 13.8 mg kg$^{-1}$ in higher-grade black phyllites. The differences in As concentrations are statistically significant (p < 0.03), and Cu, Ni, Pb and Zn are also significantly (p < 0.03) depleted in higher-grade phyllites. These differences are attributed to recrystallization of pyrite with increasing metamorphic grade, a process which introduces As and other trace elements into pore fluids, after which the high mobility of As makes it susceptible to be leached out of metapelites. Data from this study and previous research indicates that depletion of As from metapelites tends to occur once the rocks reach upper chlorite zone or lower biotite zone, corresponding to metamorphic temperatures of ~250–350 °C. This suggests that, in the absence of subsequent hydrothermal mineralization (e.g. arsenopyrite in late-stage veins), metapelites metamorphosed to upper chlorite zone or higher will be less likely to foster elevated As in groundwater compared to their lower-grade shale and slate counterparts.

© 2014 Elsevier B.V. All rights reserved.

## 1. Introduction

Groundwater in bedrock aquifers is an important drinking water source in northeastern Canada (e.g. Novakowski and Lapcevic, 1988; Cloutier et al., 2006; Kennedy and Finlayson-Bourque, 2011; Chesnaux, 2013) and the northeastern United States (e.g. Ayotte et al., 2003; Peters, 2008; DeSimone and Barbaro, 2012); for example, ~40% of the population in northern New England (USA) obtains drinking water from private bedrock wells (Ayotte et al., 2006). In this region, surveys indicate that 20–30% of private bedrock wells contain arsenic concentrations above the US Environmental Protection Agency's (USEPA) maximum contaminant level (MCL) of 10 µg/L (133 nmol/L) and the most common rock type in these aquifers is meta-sedimentary (Ayotte et al., 2006; Lipfert et al., 2006; Yang et al., 2012; Ryan et al., 2013). Consumption of drinking water with elevated arsenic is known to increase risk of bladder cancer, and this may be particularly pertinent in

* Corresponding author at: Geology Department, 276 Bicentennial Way, Middlebury College, Middlebury, VT 05753, USA. Tel.: +1 802 443 2557; fax: +1 802 443 2072.
E-mail address: pryan@middlebury.edu (P.C. Ryan).

rural New England, where bladder cancer rates exceed those for the rest of the United States (Brown et al., 1995; Ayotte et al., 2006). Elevated As in bedrock aquifers in southeastern Quebec has also been identified as a potential cause of cancer in that region (Ibanez, 2008).

An important control on the quality of water in bedrock aquifers is composition of host bedrock, and one particular concern is the presence of As-bearing pyrite or arsenopyrite, minerals which have been identified as sources in meta-sedimentary rock aquifers, particularly black shales and slates (e.g. Schreiber et al., 2003; Lipfert et al, 2006; Peters and Burkert, 2007; Ryan et al., 2013). One factor that may control abundance of As in meta-sedimentary rock aquifers is metamorphic grade. Studies indicate that As becomes depleted in meta-sedimentary rocks once they are exposed to temperatures of 250–350 °C (Bebout et al., 1999; Pitcairn et al., 2010; Large et al., 2012), a temperature interval whose upper limit roughly coincides with the metamorphic transition from chlorite zone to biotite zone (lower greenschist facies). The loss of As from rocks undergoing prograde metamorphism has been attributed to recrystallization and/or decomposition of initially As-rich diagenetic pyrite, a process which results in the formation of well-crystalline pyrite or pyrrhotite with low As content (Pitcairn et al., 2010; Large et al., 2012). This being the case, groundwater from meta-sedimentary aquifers metamorphosed to temperatures ≥250 °C is likely to be depleted in arsenic relative to groundwater produced from unmetamorphosed or weakly-metamorphosed rocks, especially black shales and slates with arsenic-rich pyrite (Peters and Burkert, 2007; Ryan et al., 2013).

In order to test the hypothesis that arsenic in metapelites becomes depleted with increasing metamorphic grade, we studied a sequence of Middle to Upper Ordovician black shale, slate and phyllite that consist of stratigraphically equivalent units which have been metamorphosed to varying degrees, from diagenetic grade black shales to black phyllites metamorphosed to uppermost chlorite zone conditions. These rocks comprise the bedrock aquifer system of the Taconic Mountain region of west-central Vermont, USA, and previous analysis in this region indicates that 22% (52/236) of private bedrock wells exceed 10 μg/L arsenic (Ryan et al., 2013). When wells are classified by metamorphic grade of host rocks, 25% of wells (51/202) producing from low-grade shales and slates of the Giddings Brook thrust slice (lower chlorite zone) exceed 10 μg/L arsenic; conversely, only 3% of wells (1/34) producing from higher-grade slates and phyllites of the Bird Mountain slice (upper chlorite zone to lowermost biotite zone; Zen, 1960) exceed 10 μg/L arsenic. By comparing bulk rock compositions from lower-grade shales and slates vs. correlative higher-grade slates and phyllites, in the context of groundwater arsenic concentrations (Ryan et al., 2013), we show that arsenic becomes depleted in metapelites during prograde regional metamorphism at temperatures of ~250–300 °C (upper chlorite zone) and that this is one of the factors that influences the concentration of arsenic in groundwater of the bedrock aquifer system.

## 2. Geology of the study area

Bedrock of the Taconic Mountain region of southwestern Vermont (Fig. 1) is characterized by Neoproterozoic to Upper Ordovician shales, slates and phyllites with minor interbedded carbonate rocks, especially in the lower part of the section (Ratcliffe et al., 2011). The sequence was originally deposited as marine mud on the Laurentian continental slope and rise prior to and during the Middle to Upper Taconian Orogeny (Zen, 1972; Landing, 2007; Ratcliffe et al., 2011) and then was deformed and metamorphosed to varying degrees during the Taconian Orogeny (Stanley and Ratcliffe, 1985) and again during the Devonian Acadian Orogeny (Chan et al., 2000).

The lowest grade (diagenetic) rocks analyzed in this study are autochthonous, largely-undeformed black and gray shales of the Austin Glen formation (Figs. 1 and 2). Slates and phyllites of the stratigraphically-equivalent Pawlet formation and underlying Poultney formation occur to the east (toward the core of the orogenic belt) in a

series of imbricated thrust slices known as the Taconic allochthons. In the study area, the Bird Mountain slice is the structurally-highest and also highest-grade (in terms of metamorphism) of the tectonic units (Zen, 1960; Goldstein et al., 2005); it was thrust over the lower-grade Giddings Brook slice, which itself was thrust onto autochthonous sedimentary rocks of the North American craton. The highest metamorphic grade in the Taconic sequence of the study area is found in the Bird Mountain slice and is placed near the boundary of the uppermost chlorite zone and the lowermost biotite zone (Zen, 1960, based on localized biotite in highest-grade metapelites). Oxygen isotope analyses of fluid inclusions in quartz–calcite strain fringes adjacent to the Bird Mountain thrust fault indicate maximum temperatures of ~250–300 °C (Goldstein et al., 2005). The dominant structural grain (cleavage planes, fold axes, fractures, thrust exposures) is primarily oriented ~north–south, and groundwater flow in the bedrock aquifer is controlled by these N–S structures as well as by bedding-parallel fractures and E–W fracture sets (Mango, 2009).

The stratigraphic and structural relationships of the upper units in the Taconic sequence of southwestern Vermont and adjacent New York State are shown in Fig. 2. The Austin Glen and Pawlet formations are Middle to Upper Ordovician (Bock et al., 1998; Ratcliffe et al., 2011) syn-orogenic (Taconian Orogeny) flysch deposits whose sedimentary parent material was a mixture of continental rise, accretionary prism, ophiolites and volcanic arc terranes (Rowley and Kidd, 1981; Garver et al., 1996; Ratcliffe et al., 2011). The Austin Glen formation is autochthonous, i.e. it has not been significantly displaced craton-ward by thrust faulting. The Pawlet formation is the higher-grade stratigraphic equivalent of the Austin Glen formation (Rowley and Kidd, 1981) in the Taconic allochthons and the Poultney formation stratigraphically underlies the Austin Glen and Pawlet formations throughout the study area. An erosional unconformity related to uplift associated with the incipient Taconian Orogeny separates the Pawlet and Poultney formations (Rowley and Kidd, 1981). Locally, the Mount Merino and Indian River formations occur as thin units between the Pawlet and Poultney formations.

## 3. Materials and methods

Data collection and analysis consisted of two main objectives: (1) determination of the chemical composition of whole rock samples (shales, slates, phyllites) and of pyrite crystals within these samples, and (2) assessment of metamorphic grade within a low-grade metamorphic terrain. These results were then combined with existing groundwater data (Ryan et al., 2013) to assess the role of low-grade metamorphism on arsenic concentrations in meta-sedimentary bedrock aquifers.

### 3.1. Bedrock sampling and analysis

Previous work has identified black and gray slates as the main source of arsenic in the Taconic region bedrock aquifer system (Ryan et al., 2013). The current study examines a suite of 30 samples of black shale, slate and phyllite bedrock – many of them with ≤3 mm pyrite crystals (i.e. visible in the field) – ranging from the Austin Glen formation in the western-most part of the study area to the Pawlet formation and (for two samples) uppermost Poultney formation in the central and eastern part of the study area (Fig. 1). Samples containing ≤5% disseminated pyrite were chosen for analysis in this study — refer to Ryan et al. (2013) for data on very pyrite-rich slates containing pyrite veins and clusters. The samples span the full range of low-grade metamorphic conditions present in the study area, from diagenetic grade in the western-most localities (Austin Glen) to uppermost chlorite zone (or lowermost biotite zone; Zen, 1960) in the eastern-most localities. Most samples were collected from freshly exposed rock in quarries or road cuts (Studwell, 2013) and samples from natural outcrops were obtained from freshly exposed surfaces and any vestiges of weathering
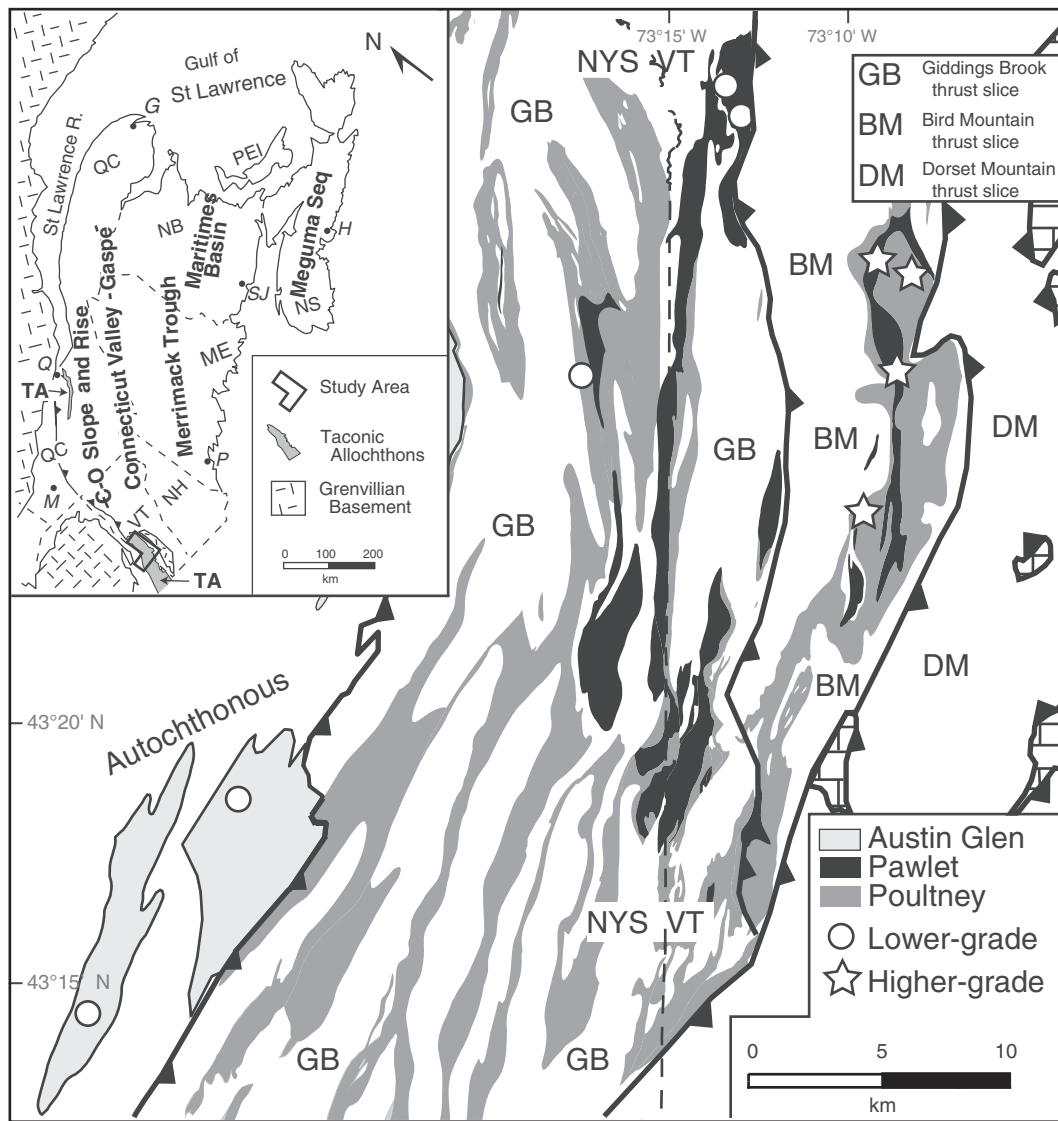
**Fig. 1.** Simplified geologic map of the study area (modified from Ratcliffe et al., 2011) emphasizing (1) map units that form the focus of this study, i.e. Austin Glen, Pawlet and Poultney formations, and (2) bedrock sample localities (circles and stars). Map areas in white are rock formations older than the Austin Glen, Pawlet and Poultney formations. "Lower grade" samples are from the autochthonous Austin Glen Fm (diagenetic grade) and lower chlorite zone Pawlet and Poultney formations within the Giddings Brook (GB) thrust slice; "higher-grade" samples are from uppermost chlorite zone Pawlet and Poultney formations within the Bird Mountain (BM) thrust slice. "Grade" refers to metamorphic grade. New York State (NYS)–Vermont (VT) border is shown. Inset: study area relative to other geologic provinces in northeastern North America, including (in bold) meta-sedimentary sequences that host bedrock aquifers throughout the region. "TA" are Taconic allochthons in the study area and near Québec City. States and provinces are shown for reference: Vermont (VT), New Hampshire (NH) and Maine (ME) in the USA and Quebec (QC), New Brunswick (NB), Prince Edward Island (PEI) and Nova Scotia (NS) in Canada. The following cities are also shown: Montreal (M), Quebec City (Q), Portland (P), Gaspe (G) and Halifax (H).

products were removed with a rock saw in the lab. The potential for variable weathering of rock samples was assessed by comparing ratios of base cations (wt.% oxide) to $Al_2O_3$ and to $TiO_2$ (Birkeland, 1999). Approximately 1 kg of rock sample was processed in a jaw crusher and shatterbox to produce fine powder, which was homogenized and split into two 5 g aliquots for chemical analysis.

Whole-rock compositions were analyzed for major elements using inductively coupled plasma-atomic emission spectrometry (ICP-AES) at Middlebury College and ICP-mass spectrometry (ICP-MS) at Acme Analytical Labs (Vancouver, BC, Canada), both cases after fusion with $LiBO_2$ and dissolution in $HNO_3$. Uncertainties determined by replicate analyses and comparison to USGS standard AGV-2 for $SiO_2$, $Al_2O_3$, $Fe_2O_3$ and CaO are $\pm 3\%$, whereas for $TiO_2$, MnO, MgO, $K_2O$, $Na_2O$ and $P_2O_5$, uncertainties are $\pm 5\%$. Uncertainties for trace elements are $\leq 10\%$ and detection limits are presented in Table 1.

Arsenic contents of various mineral phases in representative rock samples were determined by electron microprobe analysis (EMPA)

using a Cameca SX 50 electron probe with four wavelength energy dispersive spectrometers. Analytical conditions were 35 kV and 500 nA beam current. The As-Kα peak was measured using a LiF crystal and the detection limit for As was 100 ppm. The beam size was 0.25 to 0.5 μm in diameter and the standard for As was natural cobaltite containing 45.2 wt.% As, obtained from Astimex Ltd.

### 3.2. Determination of extent of low-grade metamorphism

The extent of low-grade metamorphism was quantified experimentally by using X-ray diffraction (XRD) to determine the peak breadth of the illite 001 peak from the <2 μm (equivalent spherical diameter) fraction, an approach known as the Kübler index (Kübler, 1967) or illite crystallinity index (e.g. Warr and Rice, 1994). This approach was used because changes marking increasing grade from upper diagenetic zone to upper chlorite zone of greenschist facies metamorphism occur on the microscopic or submicroscopic scale; because of this, XRD has been
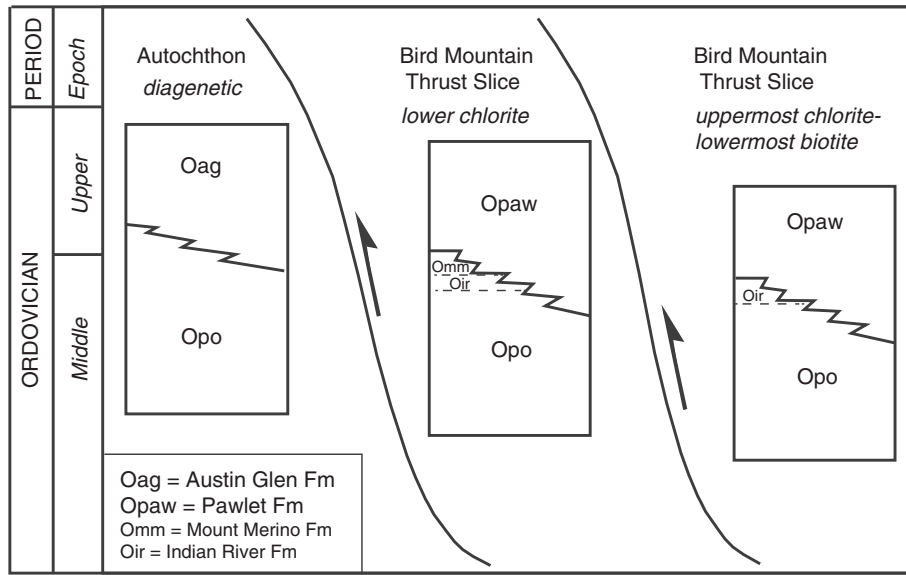
**Fig. 2.** Stratigraphy of upper Taconic sequence in the study area. Modified from Rowley and Kidd (1981) and Ratcliffe et al. (2011). Stacking of thrust sheets is shown schematically, with arrows indicating direction of thrusting.

used to quantitatively assess variability of low-grade metamorphism by measuring the progressive narrowing of the illite 001 peak that occurs with increasing grade (Wang et al., 1996). Decreasing illite peak breadth with prograde metamorphism is related to two main crystallochemical factors: (1) increasing illite X-ray scattering domain size; and (2) decreasing structural distortions in illite, including transformation of

**Table 1**
Bulk rock geochemistry. DL = detection limit. Units of concentration for major elements are wt.% oxide and for trace elements are mg kg$^{-1}$ (ppm). Oag = Austin Glen formation, Opaw = Pawlet formation, Opo = Poultney formation.

| Sample | Fm | SiO$_2$ | TiO$_2$ | Al$_2$O$_3$ | Fe$_2$O$_3$ | MnO | MgO | CaO | Na$_2$O | K$_2$O | LOI | SUM | As | Cu | Pb | Zn | Ni | Th | U |
|---|---|---|---|---|---|---|---|---|---|---|---|---|---|---|---|---|---|---|---|
| DL | | 0.01 | 0.01 | 0.01 | 0.04 | 0 | 0.01 | 0.01 | 0.01 | 0.01 | 0.1 | | 0.5 | 0.1 | 0.1 | 1.0 | 0.1 | 0.2 | 0.1 |
| *Higher-grade samples from Bird Mountain thrust slice (upper chlorite grade)* | | | | | | | | | | | | | | | | | | | |
| 092712-1 | Opaw | 61.4 | 0.86 | 15.9 | 6.32 | ND | 2.82 | 0.17 | 1.91 | 4.96 | 5.4 | 99.8 | 13.4 | 34.7 | 9.5 | 61 | 18.6 | 10.5 | 3.4 |
| 092712-2 | Opaw | 62.4 | 0.92 | 17.0 | 4.11 | ND | 2.64 | 0.15 | 2.20 | 5.32 | 4.7 | 99.4 | 10.4 | 9.0 | 20.6 | 16 | 10.0 | 11.0 | 3.9 |
| 092712-3 | Opaw | 59.7 | 0.96 | 16.6 | 5.75 | ND | 3.13 | 0.40 | 2.47 | 4.86 | 5.4 | 99.3 | 12.3 | 28.2 | 11.7 | 82 | 29.2 | 12.3 | 4.3 |
| 092712-4 | Opaw | 62.3 | 0.92 | 15.8 | 6.00 | ND | 2.49 | 0.17 | 3.28 | 4.03 | 4.3 | 99.3 | 17.0 | 31.4 | 36.0 | 78 | 23.8 | 11.9 | 4.4 |
| 092712-7 | Opaw | 71.7 | 0.47 | 11.0 | 4.31 | ND | 1.55 | 0.09 | 0.90 | 4.07 | 5.8 | 99.9 | 16.1 | 13.2 | 16.9 | 5 | 1.5 | 6.0 | 4.1 |
| 092712-8 | Opaw | 74.4 | 0.50 | 8.89 | 5.06 | ND | 1.25 | 0.05 | 0.67 | 3.27 | 5.6 | 99.7 | 17.5 | 22.6 | 18.7 | 7 | 1.6 | 5.7 | 5.5 |
| 092712-9 | Opaw | 75.6 | 0.47 | 8.99 | 3.95 | 0.00 | 1.36 | 1.86 | 0.92 | 3.02 | 3.7 | 99.9 | 10.9 | 39.1 | 16.9 | 56 | 15.8 | 6.6 | 7.2 |
| 092712-10 | Opaw | 73.7 | 0.54 | 9.16 | 4.99 | ND | 1.28 | 0.07 | 0.74 | 3.36 | 5.5 | 99.3 | 16.4 | 19.7 | 22.7 | 12 | 4.1 | 7.9 | 9.0 |
| 092712-11 | Opo | 86.3 | 0.26 | 6.20 | 0.76 | ND | 0.53 | 0.06 | 0.36 | 2.08 | 2.7 | 99.3 | 11.7 | 6.2 | 10.8 | 9 | 6.8 | 3.9 | 6.1 |
| 092712-12 | Opaw | 85.0 | 0.33 | 7.24 | 1.37 | ND | 0.55 | 0.05 | 0.31 | 2.39 | 2.6 | 99.9 | 18.6 | 18.1 | 14.9 | 24 | 7.0 | 4.1 | 5.7 |
| 092712-13 | Opo | 85.8 | 0.29 | 6.85 | 0.66 | ND | 0.53 | 0.08 | 0.34 | 2.31 | 3.0 | 99.9 | 12.0 | 3.2 | 12.5 | 6 | 3.9 | 4.3 | 6.6 |
| 092712-14 | Opaw | 71.5 | 0.56 | 12.5 | 4.45 | 0.02 | 3.18 | 0.45 | 2.40 | 2.12 | 2.8 | 100 | 1.1 | 13.1 | 12.3 | 77 | 33.0 | 7.7 | 0.9 |
| 092712-15 | Opaw | 64.3 | 0.75 | 16.2 | 4.90 | 0.04 | 3.66 | 0.29 | 1.52 | 3.84 | 3.6 | 99.2 | 1.1 | 18.3 | 6.0 | 88 | 35.2 | 9.2 | 1.2 |
| 092712-18 | Opaw | 48.3 | 1.23 | 23.5 | 9.17 | 0.03 | 3.25 | 0.24 | 1.91 | 5.81 | 5.6 | 99.1 | 18.2 | 39.7 | 21.0 | 92 | 40.1 | 17.3 | 3.3 |
| 092712-19 | Opaw | 75.1 | 0.34 | 9.17 | 5.08 | 0.01 | 0.99 | 0.12 | 0.44 | 3.06 | 5.3 | 99.6 | 30.3 | 59.1 | 21.7 | 61 | 48.1 | 5.0 | 6.3 |
| Mean | | 70.5 | 0.63 | 12.3 | 4.46 | 0.02 | 1.95 | 0.28 | 1.36 | 3.63 | 4.41 | | 13.8 | 23.7 | 16.8 | 44.9 | 18.6 | 8.2 | 4.8 |
| St. Dev | | 10.8 | 0.3 | 5.0 | 2.2 | 0.0 | 1.1 | 0.5 | 0.9 | 1.2 | 1.2 | | 7.1 | 15 | 7.3 | 34 | 15 | 3.8 | 2.2 |
| *Lower-grade samples from autochthonous zone and Giddings Brook thrust slice (<lower chlorite grade)* | | | | | | | | | | | | | | | | | | | |
| 092012-4 | Oag | 60.1 | 0.63 | 13.6 | 10.7 | 0.03 | 2.98 | 1.24 | 1.45 | 3.67 | 5.2 | 99.5 | 10.2 | 43.7 | 19.5 | 79 | 36.8 | 12.1 | 4.1 |
| 092012-5 | Oag | 61.0 | 0.81 | 17.0 | 7.37 | 0.07 | 2.40 | 0.15 | 1.39 | 3.82 | 5.7 | 99.8 | 11.6 | 44.7 | 30.3 | 93 | 39.4 | 13.4 | 4.3 |
| 092012-11 | Oag | 64.6 | 0.66 | 13.1 | 7.44 | 0.04 | 2.62 | 0.21 | 1.71 | 3.25 | 6.2 | 99.8 | 15.2 | 54.5 | 15.8 | 79 | 22.0 | 11.0 | 9.2 |
| 092012-12 | Oag | 55.6 | 0.81 | 16.7 | 7.46 | 0.03 | 4.40 | 1.92 | 1.50 | 4.63 | 6.3 | 99.4 | 43.7 | 30.8 | 17.8 | 33 | 20.1 | 11.8 | 8.4 |
| 092012-13 | Oag | 68.8 | 0.51 | 10.4 | 4.35 | 0.02 | 2.00 | 0.43 | 2.12 | 2.19 | 8.4 | 99.2 | 21.6 | 64.5 | 30 | 71 | 34.1 | 8.6 | 6.8 |
| 100412-11 | Oag | 64.5 | 0.73 | 15.0 | 4.35 | 0.01 | 2.48 | 0.47 | 1.38 | 7.55 | 3.0 | 99.4 | 37.9 | 35.6 | 26.9 | 52 | 36.0 | 10.5 | 5.1 |
| 112912-1 | Opaw | 61.6 | 0.78 | 16.0 | 6.74 | 0.06 | 2.26 | 0.14 | 1.45 | 3.46 | 7.1 | 99.6 | 40.0 | 80.3 | 33.2 | 169 | 79.2 | 11.4 | 6.2 |
| 112912-2 | Opaw | 62.1 | 0.72 | 14.5 | 6.24 | 0.01 | 2.66 | 0.11 | 1.79 | 3.81 | 7.9 | 99.9 | 51.7 | 52.4 | 36.7 | 100 | 60.6 | 8.1 | 7.1 |
| 112912-3 | Opaw | 61.2 | 0.73 | 14.0 | 7.57 | 0.03 | 3.34 | 1.38 | 1.93 | 3.72 | 5.5 | 99.4 | 27.9 | 69.5 | 30.2 | 109 | 39.7 | 10.9 | 6.6 |
| 112912-4 | Opaw | 59.1 | 0.78 | 17.1 | 6.32 | 0.01 | 3.38 | 0.15 | 1.66 | 4.48 | 6.9 | 99.9 | 38.5 | 63.8 | 40 | 85 | 57.9 | 9.8 | 9.6 |
| 112912-5 | Opaw | 59.3 | 0.79 | 16.3 | 6.83 | 0.01 | 3.68 | 0.62 | 1.64 | 4.44 | 6.1 | 99.7 | 37.6 | 48 | 45.7 | 147 | 105 | 11.4 | 8.9 |
| 112912-6 | Opaw | 66.1 | 0.47 | 10.4 | 4.83 | 0.05 | 3.46 | 3.50 | 1.85 | 2.42 | 6.5 | 99.7 | 18.6 | 91.5 | 13.9 | 124 | 50.8 | 9.6 | 6.4 |
| 112912-8 | Opaw | 60.4 | 0.68 | 15.3 | 9.05 | 0.01 | 3.12 | 0.14 | 1.35 | 4.22 | 5.2 | 99.4 | 36.0 | 33.5 | 31.3 | 153 | 56.5 | 6.7 | 5.0 |
| 112912-9 | Opaw | 52.6 | 1.28 | 23.1 | 7.50 | 0.05 | 2.61 | 0.43 | 1.13 | 5.95 | 5.3 | 99.9 | 7.6 | 71.5 | 27.5 | 126 | 57.8 | 16.7 | 4.1 |
| 112912-10 | Opaw | 64.3 | 0.79 | 13.8 | 6.51 | 0.11 | 1.93 | 3.06 | 1.57 | 3.01 | 4.7 | 99.8 | 5.6 | 40.3 | 16 | 97 | 39.9 | 9.5 | 3.0 |
| Mean | | 61.4 | 0.74 | 15.1 | 6.88 | 0.04 | 2.89 | 0.93 | 1.60 | 4.04 | 6.00 | | 26.9 | 55 | 27.7 | 101 | 49.0 | 10.8 | 6.3 |
| St. Dev | | 4.0 | 0.2 | 3.0 | 1.7 | 0.0 | 0.7 | 1.1 | 0.3 | 1.3 | 1.3 | | 14.9 | 18 | 9.5 | 38 | 22 | 2.4 | 2.1 |

expandable 2:1 layers to illite 2:1 layers with interlayer $K^+$. Note: following convention (e.g. Warr and Rice, 1994; Wang et al., 1996), the term "illite" is used in this study to refer to all aluminous 2:1 K-micas, from low expandability illite that occurs in shales to incipient muscovite that occurs in slates and phyllites.

Rock samples were disaggregated with a hammer and sieved to <850 μm, then approximately 50 g was added to 150 mL of distilled water and disaggregated using a Branson 450 sonifer. The <2 μm fraction (equivalent spherical diameter; ESD) was collected by timed sedimentation in Atterberg cylinders after adding 0.2 g of sodium pyrophosphate as a deflocculating agent. Oriented mounts were prepared from suspensions of the <2 μm fraction of all 30 samples by sedimentation of clay slurry onto a glass slide, and slides were dried overnight at 60 °C. Mineralogical analysis was conducted on air-dried preparations using a Bruker D8 Advance diffractometer at Middlebury College with analytical conditions of 1.2 °2θ/s at 40 kV and beam current of 40 μA. Bruker EVA© software was used to measure the full width at half maximum (FWHM) (in units of °2θ) of the illite 001 peak at 10 Å, and FWHM values were used as a proxy for illite crystallinity and, by extension,

degree of low-grade metamorphism (Wang et al., 1996). In order to constrain metamorphic grade as precisely as possible, measurements of the Kübler index/illite crystallinity were compared to field- and XRD-based observations of Zen (1960), and also to $\delta^{18}O$ values of quartz and calcite in metamorphic veins determined by Goldstein et al. (2005).

### 3.3. Statistical analysis

Independent variable Mann–Whitney U-tests were conducted on trace element concentrations between two sample sets (15 samples each), one with lower-grade (<lower chlorite zone) and one containing the higher grade phyllites (>upper chlorite zone), in order to determine if there are statistically significant differences in means between the two populations. Similarities in depositional environment and parent sediment composition (Rowley and Kidd, 1981) imply that differences in composition should be related to superimposed diagenetic and/or metamorphic processes.

Principal component analysis (PCA) was used to summarize the variation in bulk rock geochemistry across the sites. Because the
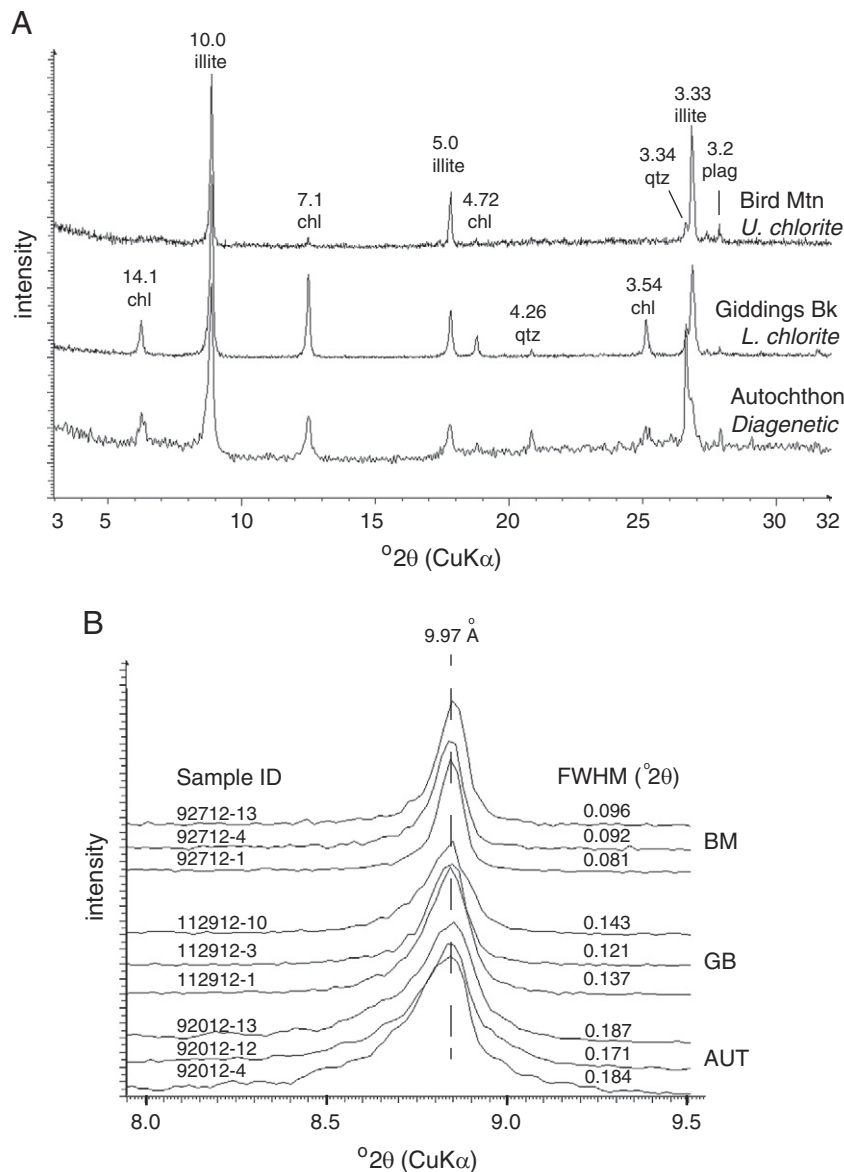


**Fig. 3.** XRD patterns for <2 μm fraction of oriented, air-dried mounts of representative samples. (A) mineralogy of Pawlet formation phyllite (>upper chlorite zone) from the Bird Mountain (BM) thrust slice, Pawlet formation slate (lower chlorite zone) from the Giddings Brook (GB) thrust slice, and autochthonous (AUT) Austin Glen shale (diagenetic grade); (B) the illite 001 peak for representative samples from the three main structural zones. Note decreasing peak breadth (FWHM) with increasing grade.

**Table 2**
Measurements of full width at half-maximum (FHWM) of illite 001 peak (10 Å) and chlorite 001 (14.1 Å) and chlorite 002 (7.1 Å) peaks (in °2θ). Where indicated as "–", chlorite peaks were absent or too weak to be measured in XRD patterns. Also shown is As concentration (ppm) in bulk rock. TZ = tectonic zone (AUT = autochthonous, GB = Giddings Brook slice and BM = Bird Mountain slice).

| Diagenetic to lower chlorite grade | | | | | | Upper chlorite to lower biotite grade | | | | | |
|---|---|---|---|---|---|---|---|---|---|---|---|
| Sample | Fm | TZ | I (001) | Chl (002) | As | Sample | TZ | Fm | I (001) | Chl (002) | As |
| 092012-4 | Oag | AUT | 0.190 | 0.132 | 10.2 | 092712-1 | BM | Opaw | 0.081 | – | 13.4 |
| 092012-5 | Oag | AUT | 0.152 | 0.123 | 11.6 | 092712-2 | BM | Opaw | 0.107 | – | 10.4 |
| 092012-11 | Oag | AUT | 0.131 | 0.152 | 15.2 | 092712-3 | BM | Opaw | 0.113 | – | 12.3 |
| 092012-12 | Oag | AUT | 0.171 | 0.113 | 43.7 | 092712-4 | BM | Opaw | 0.092 | – | 17.0 |
| 092012-13 | Oag | AUT | 0.187 | 0.147 | 21.6 | 092712-7 | BM | Opaw | 0.092 | – | 16.1 |
| 100412-11 | Oag | AUT | 0.138 | 0.144 | 37.9 | 092712-8 | BM | Opaw | 0.110 | – | 17.5 |
| 112912-1 | Opaw | GB | 0.137 | 0.087 | 40.0 | 092712-9 | BM | Opaw | 0.074 | – | 10.9 |
| 112912-2 | Opaw | GB | 0.136 | 0.110 | 51.7 | 092712-10 | BM | Opaw | 0.096 | – | 16.4 |
| 112912-3 | Opaw | GB | 0.121 | 0.094 | 27.9 | 092712-11 | BM | Opo | 0.103 | – | 11.7 |
| 112912-4 | Opaw | GB | 0.184 | 0.118 | 38.5 | 092712-12 | BM | Opaw | 0.100 | – | 18.6 |
| 112912-5 | Opaw | GB | 0.127 | 0.102 | 37.6 | 092712-13 | BM | Opo | 0.096 | – | 12.0 |
| 112912-6 | Opaw | GB | 0.121 | 0.101 | 18.6 | 092712-14 | BM | Opaw | 0.089 | 0.074 | 1.1 |
| 112912-8 | Opaw | GB | 0.135 | 0.114 | 36.0 | 092712-15 | BM | Opaw | 0.101 | 0.079 | 1.1 |
| 112912-9 | Opaw | GB | 0.144 | 0.095 | 7.6 | 092712-18 | BM | Opaw | 0.104 | 0.089 | 18.2 |
| 112912-10 | Opaw | GB | 0.143 | 0.126 | 5.6 | 092712-19 | BM | Opaw | 0.082 | 0.086 | 30.3 |
| Mean | | | 0.148 | 0.117 | 26.9 | Mean | | | 0.096 | 0.082 | 13.8 |
| St. Dev | | | 0.024 | 0.020 | 14.9 | St. Dev | | | 0.011 | 0.007 | 7.1 |

geochemical data had very different variances, all properties were standardized to the unit variance by using the correlation matrix rather than the covariance matrix. This analysis was conducted in R version 3.0.1 (R Core Team 2013, R Foundation for Statistical Computing. Vienna, Austria).

# 4. Results

## 4.1. Mineralogy and illite crystallinity

XRD analysis of the <2 μm fraction indicates that shales from the Austin Glen formation and slates from the Pawlet and Poultney formations in the Giddings Brook slice contain illite and chlorite with minor quartz and plagioclase. This mineralogical assemblage is typical of pelitic rocks from upper diagenetic grade to low-grade metamorphic conditions (i.e. chlorite zone of the greenschist facies). Phyllites from the Pawlet and Poultney formations in the higher-grade Bird Mountain slice are mineralogically similar but contain less chlorite in the <2 μm fraction than those of lower-grade shales and slates (Fig. 3; Table 1), likely reflecting increasing grain size with prograde metamorphism (Zen, 1960). In general, phyllites from the Bird Mountain slice are notably coarser-grained (e.g. visible "sericitic" micas) than the lower-grade shales and slates and the phyllites also contain deformed 1–5 mm wide quartz veins that do not occur in the finer-grained shales and slates of the autochthonous zone or Giddings Brook slice. Similar observations were made by Zen (1960).

Measurements of FWHM of the illite 001 peak (Table 2) document decreasing peak breadth (increasing illite crystallinity) with increasing grade, from (A) Austin Glen formation shales in the autochthonous zone (mean FHWM = 0.162 ± 0.025 °2θ) to (B) Pawlet formation slates in the Giddings Brook slice (mean FHWM = 0.139 ± 0.019 °2θ) to (C) Pawlet and Poultney formation phyllites in the Bird Mountain slice (mean FHWM = 0.97 ± 0.010 °2θ).

Because of similar means and extensive overlap in illite 001 FWHM values for Austin Glen shales and Pawlet formation slates from the Giddings Brook slice, these two units were grouped together as "lower-metamorphic grade" samples, whereas the coarser-grained phyllites from the Pawlet and Poultney formations in the Bird Mountain slice are grouped together as "higher-metamorphic grade" samples (Tables 1 and 2). These groupings are generally consistent with observations of Zen (1960), who documented the localized presence of biotite in phyllites of the Bird Mountain slice (and its absence in lower-grade shales and slates) and also interpreted the difference in grain size of relatively coarse phyllites compared to fine-grained shales and

slates as qualitative evidence of higher grade conditions in the Bird Mountain phyllites versus lower-grade shales and slates. FWHM of the chlorite 002 peak is shown for comparison (Table 2), and while it also decreases with increasing grade, chlorite crystallinity is a less reliable indicator of low-grade metamorphism than illite is (Wang et al, 1996).

## 4.2. Bulk rock geochemistry

Major element compositions of Austin Glen shales and Pawlet and Poultney formation slates and phyllites are very similar (Table 1). The main difference in major elements is higher mean $SiO_2$ in higher-metamorphic grade phyllites compared to shales and slates, which is mainly due to the presence of thin (<5 mm) quartz veins in three of the higher-grade rocks (e.g. 92712-11, 12, 13). Statistical analysis indicates that there is no significant difference in major element concentrations between lower-grade and higher-grade sample groups (independent variable Mann–Whitney U-tests); what is also important to note is that lower-grade vs. higher-grade sample sets exhibit no significant difference in rare earth element (REE) concentrations and nearly all other trace element concentrations are not significantly different among the two sample sets. REE abundance normalized to North
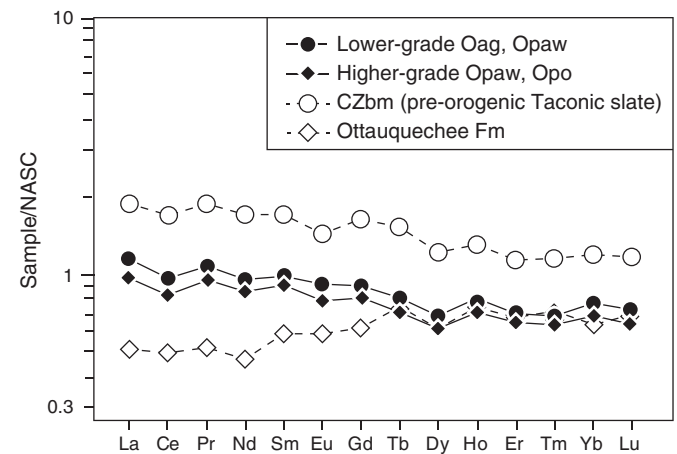


**Fig. 4.** REEs normalized to NASC (mass basis), illustrating similarity in composition of samples from the current study (dark symbols) compared to a suite of samples from the Mettawee Shale Member of the Bull formation (CZbm) (lower part of Taconic sequence in the study area; Thompson, 2011) and from the Cambrian Ottauquechee formation of north-central Vermont (Anderson, 2006). Data shown are average value for each suite.
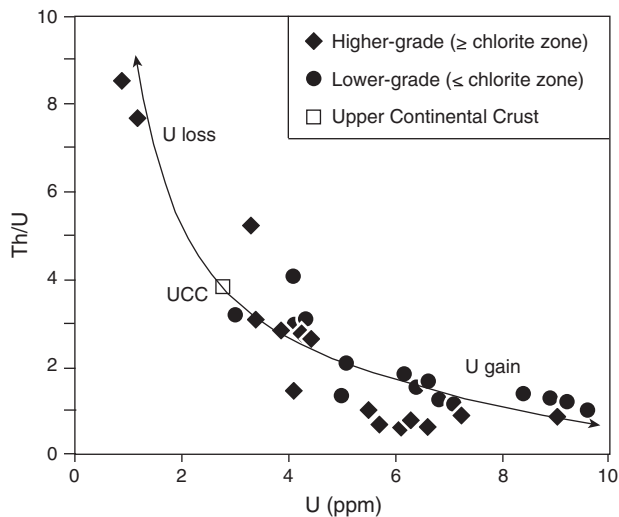
**Fig. 5.** U vs. Th/U. Curve is a model for U loss or gain from mean upper continental crust (UCC) (adopted from Hurowitz and McLennan, 2005). Note overlap of higher-grade and lower-grade samples analyzed herein. Values are calculated on a mass basis.

American shale composite (NASC; Gromet et al., 1984) indicates a nearly identical pattern for lower-grade vs. higher-grade sample sets, especially when compared to other slates and phyllites from the region (Fig. 4), and a plot of U vs. Th/U (after Hurowitz and McLennan, 2005) shows no systematic difference between lower-grade vs. higher-grade sample sets (Fig. 5). The two samples that plot outside of the range of

the rest are 92712-14 and 92712-15, both of which are Pawlet formation slates that are also low in As, Pb and Sb but otherwise are compositionally indistinguishable from the other 28 samples.

Based on independent variable Mann–Whitney U-tests, the only elements whose concentrations are significantly different among the two sample sets are As, Cu, Ni, Pb and Zn (Figs. 6 and 7), each of which is significantly depleted in higher-grade rocks relative to lower-grade rocks. Concentrations of these five trace elements in higher-grade rocks are ~50% of values in lower-grade rocks, and dispersion about the mean in higher-grade rocks is appreciably lower than that in lower-grade rocks (Figs. 6 and 7).

Results of PCA analysis indicate that the first and second principal component axes explain 43.6% and 13.6% of the variation in bulk rock geochemistry, respectively. In particular, the trace elements As, Cu, Ni, Pb, Sb, Se, U and Zn are separated by principal component 2 (PC2) in the direction of lower-grade samples, correlating to their greater abundance of these samples (Fig. 8); by comparison, only $SiO_2$ is appreciably separated by PC2 in the direction of higher-grade rocks, likely reflecting occurrence of thin quartz veins in three higher-grade samples (92712-11, 12, 13).

### 4.3. Electron microprobe analysis

Element plots for S, Fe and S as well as a backscattered electron (BSE) image of a pyrite-rich zone of a slate sample (112912-2) from the Pawlet formation is shown in Fig. 9. Increased brightness in some zones within the pyrite is caused by substitution of As into pyrite to concentrations as high as 1.54 wt.% (15,400 ppm) As in $FeS_2$.
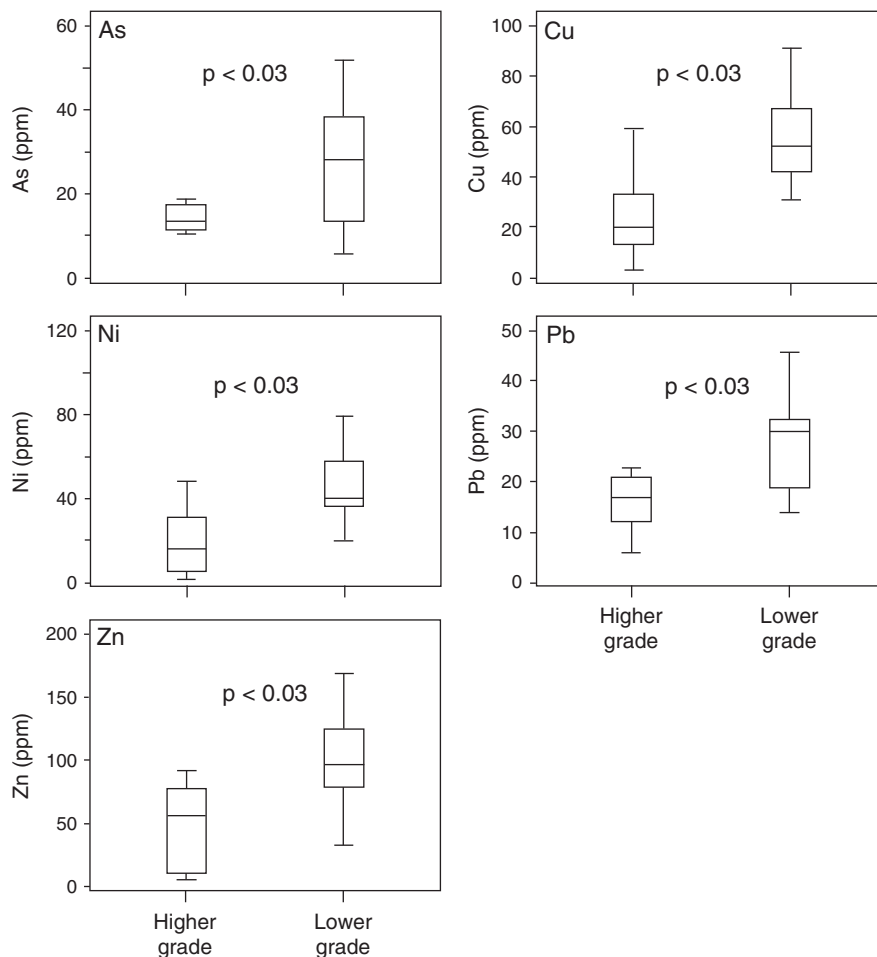


**Fig. 6.** Box and whisker diagrams of As, Cu, Ni, Pb and Zn illustrating depletion of mobile trace elements in higher-grade rocks.
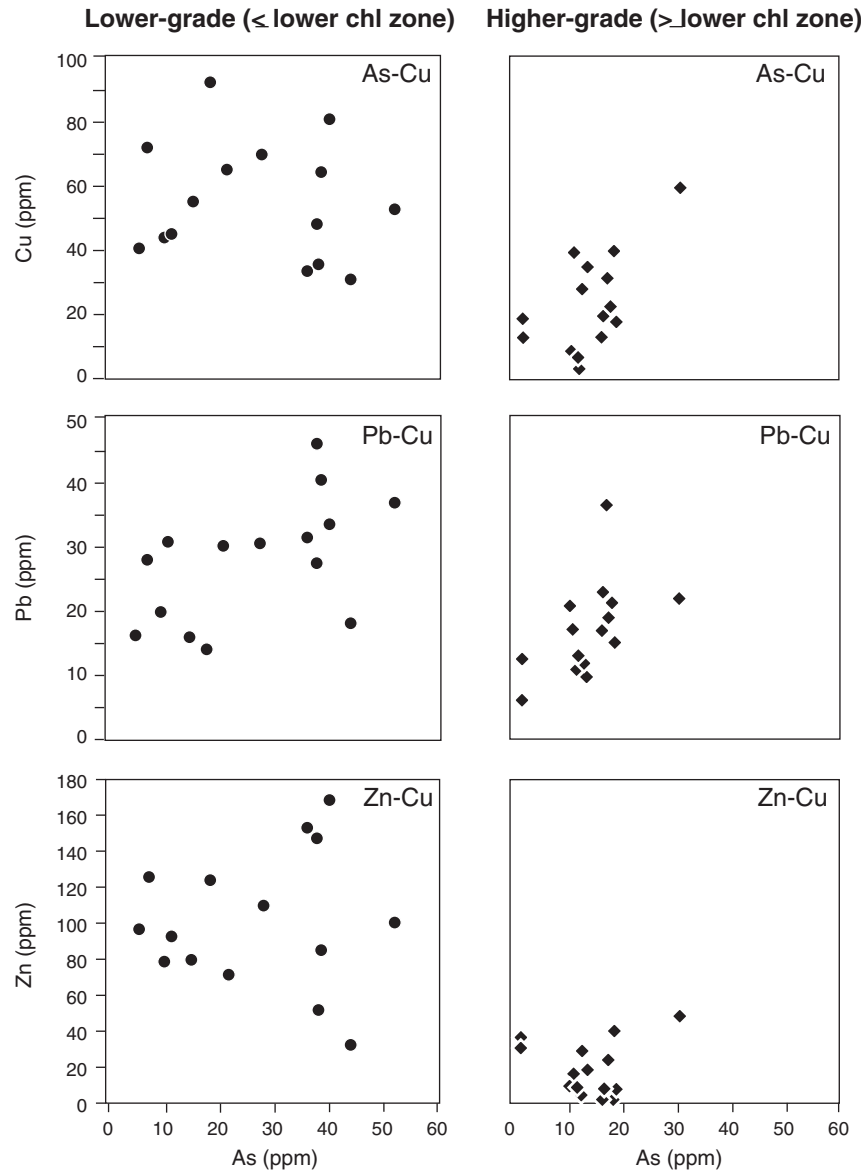
**Fig. 7.** Bivariate plots of As vs. Cu, As vs. Pb and As vs. Zn for lower-grade and higher-grade rocks.

Results of EMPA spot analyses (Fig. 10) reveal an inverse relationship of As to S, consistent with substitution of As for S in pyrite, which can be expressed as: $(SAs)^{-2} = S_2^{-2}$. The co-precipitation of As into pyrite is consistent with previous studies documenting As content in pyrite at concentrations of up to 10 wt.% (Kolker and Nordstrom, 2001; Abraitis et al., 2004), a level above which the system will form separate phases of pyrite + arsenopyrite (FeAsS) (Reich and Becker, 2006). Concentrations of As in pyrite from a higher-grade phyllite were below detection limit (100 ppm) so probe data for higher-grade pyrite is not presented.

## 5. Discussion

The main controls on the abundance of As and other trace elements in sedimentary and meta-sedimentary rocks are (1) initial sediment composition, and (2) post-depositional modifications to the original sediment, including diagenetic, metamorphic or hydrothermal alterations to mineral assemblage or bulk composition. Regarding the upper strata of the Taconic allochthons (Pawlet formation and the uppermost Poultney formation) and correlative autochthonous strata (Austin Glen formation), sediments were derived from a mixed source

influenced by inputs from the Laurentian craton to the west, an approaching arc to the east (relative to present day coordinates), and up-thrusted and recycled sediments previously deposited on the eastern margin of Laurentia (Rowley and Kidd, 1981; Hurowitz and McLennan, 2005). These correlative units were deposited in the basin formed by Laurentia to the west and the Taconian arc to the east, and petrographic analysis by Rowley and Kidd (1981) and geochemical analyses of Hurowitz and McLennan (2005) as well as REE and other trace elements reported herein imply a relatively uniform initial sediment composition in these units.

Various lines of geochemical evidence indicate that initial sediment composition of the lower-grade and higher-grade rocks studied herein was uniform. REEs normalized to NASC (Fig. 4) are nearly identical for lower-grade and higher-grade Austin Glen–Pawlet–Poultney samples and their patterns are distinguished from older metapelites from the region. A plot of U vs. U/Th (Fig. 5) also demonstrates the geochemical affinities of lower-grade and higher-grade samples analyzed, and PCA analysis (Fig. 8) shows that the immobile REEs are tightly clustered and close to the origin, reflecting their similar abundances in lower-grade and higher-grade samples. The possibility that chemical weathering may have affected concentrations of As or other elements
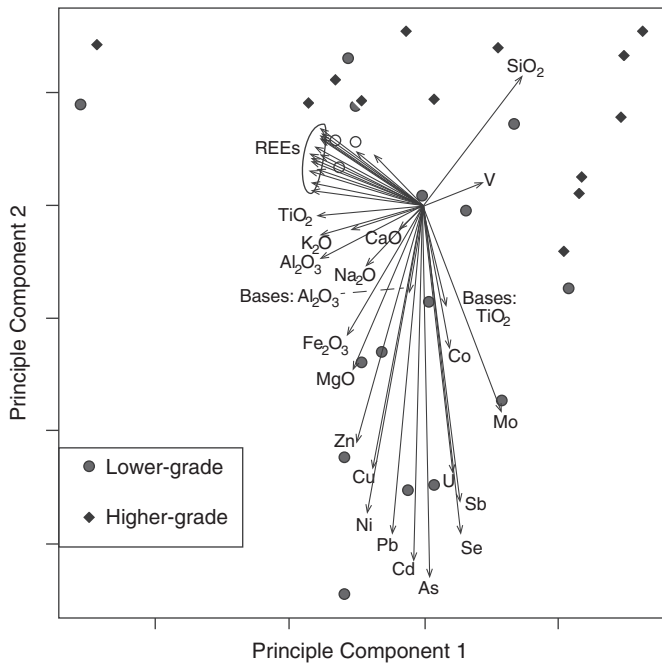
**Fig. 8.** Biplot for principal component analysis. Lower-grade sites are represented by circles and higher-grade sites by diamonds. Loadings for different geochemical parameters are shown with the labeled arrows.
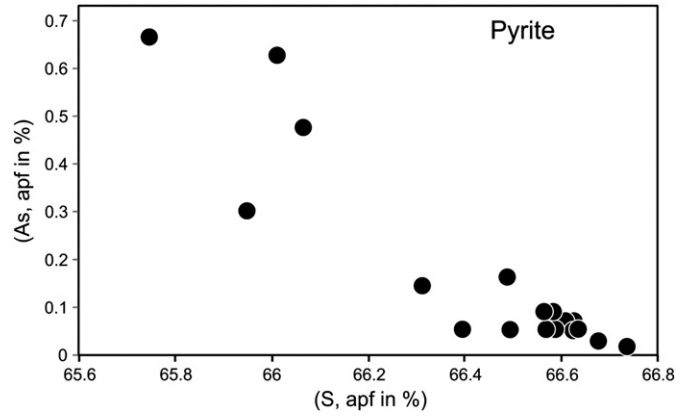


**Fig. 10.** As and S in atom per formula unit of pyrite crystals in the same sample as those in Fig.9.

in lower-grade vs. higher-grade rocks analyzed in this study is unlikely given the very similar ratios of base cations (wt.% oxides) to $TiO_2$ and to $Al_2O_3$ (Birkeland, 1999) for both sample suites — the ratios of base cations: $TiO_2$ and of base cations: $Al_2O_3$ are plotted in the PCA analysis (Fig. 8) and their locations close to the origin are consistent with a lack of weathering effect on geochemistry.

Thus, the following lines of evidence indicate that pre-metamorphic concentrations of As were the same for the lower-grade vs. higher-grade samples analyzed in this study: (1) Austin Glen–Pawlet formation sediments were derived from the same source and should be effectively compositionally identical; (2) the anoxic/dysoxic depositional environment that fostered black shale formation was similar for all of the
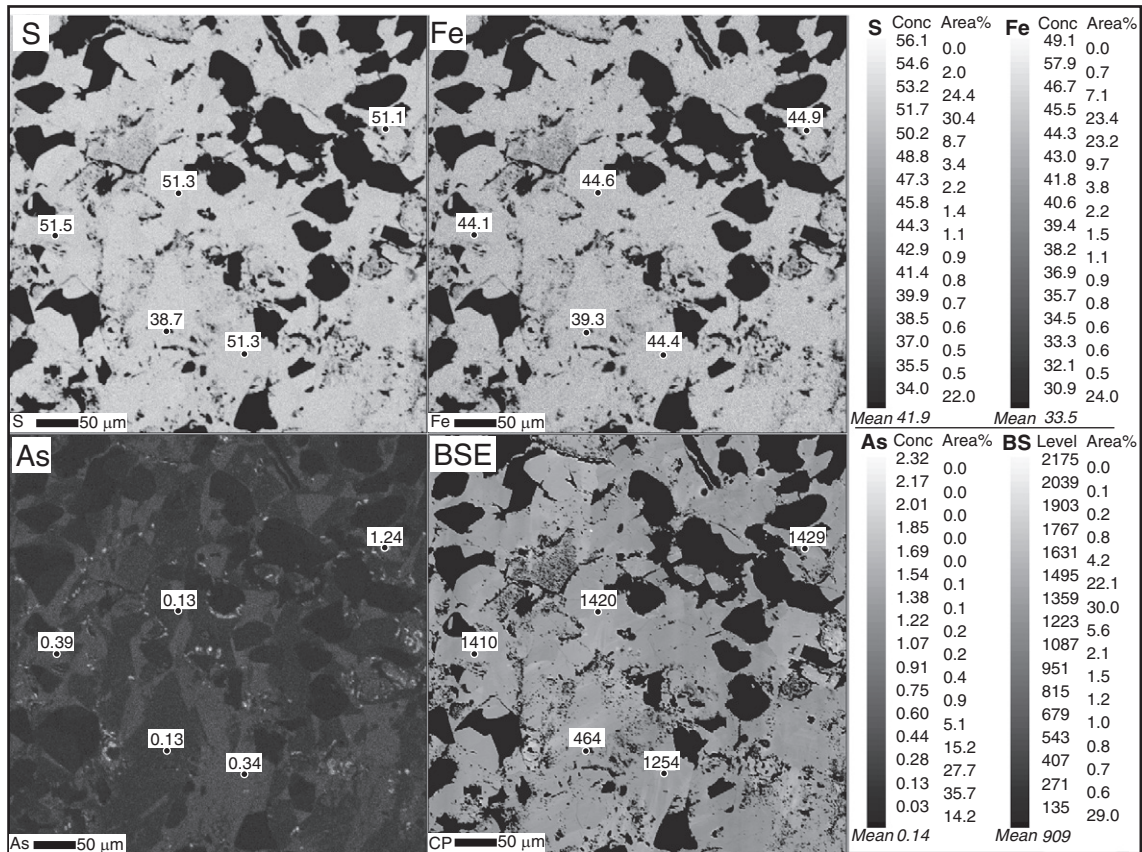


**Fig. 9.** X-ray maps for SKα, FeKα and AsLα, and a BSE image of pyrite-rich zone within a Pawlet formation slate. Brighter areas in the X-ray maps indicate higher concentrations, and concentrations for individual spot analyses are shown (in wt.%). Dark grains are quartz.

samples analyzed in this study; and (3) major and trace element indicators of sediment composition (with the exception of trace elements such as As, Cu, Ni, Pb and Zn) indicate a similarity in pre-metamorphic compositions across the sample sets. If this is the case, depletion of As, Cu, Ni, Pb and Zn began to occur in the upper chlorite zone of greenschist facies metamorphism approaching temperatures of 250–300 °C (based on $\delta^{18}$O data of Goldstein et al., 2005).

Syn-depositional biogeochemical conditions at the sediment–seawater interface may exert a strong influence on sediment composition, particularly redox conditions and their effect on redox-sensitive trace elements, including As and U. Periods of marine anoxia and dysoxia in the closed marine basin associated with deposition of the black pelites of the upper Taconic strata (Landing, 2007) tend to foster fixation of As and other trace elements into early diagenetic iron sulfides (Large et al., 2012), helping to explain high As concentrations typically associated with black shales (Smedley and Kinniburgh, 2002).

Post-depositional controls on arsenic content of black shales and related pelitic rocks begin with early-stage diagenetic recrystallization of arsenic-rich amorphous iron sulfides (e.g. mackinawite, ~FeS) into framboidal or euhedral pyrite that preserves high arsenic concentrations (Scholz and Neumann, 2007; Large et al., 2012); subsequently, with increasing temperatures from diagenetic grade into lower greenschist facies conditions, pyrite undergoes renewed episodes of recrystallization that cause As (and other mobile elements, e.g. Cu, Pb, Zn) to be leached from metapelites, resulting in phyllites and schists with low arsenic content relative to their low-grade shale and slate equivalents (Bebout et al., 1999; Large et al., 2012). The mobilization of arsenic and other mobile elements (e.g. B, Cu, Mo, Ni, Pb, Sb, Zn) out of pelitic rocks often results in hydrothermal veins or shear zones with high arsenic content (Large et al., 2012), and in some orogenic belts leached As is fixed into ultramafic rocks while they undergo serpentinization (Hattori et al., 2005).

If the Taconic sequence of eastern New York State and western Vermont serves as a general model for the behavior of arsenic during metamorphism of pelitic rocks, it is likely that aquifers whose composition is influenced by low-grade black shales and slates (<chlorite zone) are at greater risk of elevated arsenic than are comparable aquifers influenced by rocks metamorphosed to conditions greater than or equal to the upper chlorite zone (~≥250 °C). Data from the Taconic Mountain bedrock aquifer system are consistent with this hypothesis: 25% of wells producing from low-grade shales and slates exceed 10 μg/L arsenic, whereas only 3% of wells producing from higher-grade slates and phyllites exceed 10 μg/L arsenic (Ryan et al., 2013). Similar sequences occur throughout northeastern North America and preliminary data from the variably-metamorphosed Connecticut Valley–Gaspe sequence of Quebec and Vermont are consistent with this hypothesis: arsenic-bearing black shales and slates in southeastern Quebec are spatially related to elevated groundwater arsenic; by comparison, As-depleted schists in NE Vermont (biotite and garnet zone) are spatially associated with low-arsenic groundwater (Ryan et al., 2012). Similar observations were made by O'Shea et al. (2008) in variably metamorphosed rocks of Maine. It is important to note that bedrock geology is only one of many parameters that controls groundwater As; for example, Yang et al. (2012) developed a model to predict As concentration in groundwater in southern Maine (New England, USA) and found that occurrences of elevated As in groundwater were best-predicted by models that incorporate bedrock geology as well as pH.

Not all meta-pelitic rock sequences follow the relatively straightforward transition observed in the Taconic Mountain region, notably some examples of As-rich high-grade rocks affected by hydrothermal and metasomatic influences. West et al. (2008) documented a mean As concentration of 330 ppm in amphibolite-facies Fe–Mn-rich rocks (Wilson Cove Member of the Cushing formation, Maine) where the As occurs in arsenopyrite and loellingite in metamorphosed marine clastic sediments and hydrothermal exhalatives. Lipfert (2006) determined a

mean As concentration of 68 ppm in amphibolite-facies metapelites (Penobscot formation, Maine) whose protolith was black shale; in this sequence, however, As occurs in arsenopyrite hosted by late-stage quartz–calcite–tourmaline hydrothermal veins rather than as diagenetic pyrite. In northern Vermont, metasomatized As-rich antigorite and magnesite in serpentinites serve as a localized groundwater As source in a region otherwise dominated by As-poor biotite and garnet zone metapelites (Ryan et al., 2011). While these three examples of As-rich high-grade metamorphic rocks may serve as models for regions locally affected by hydrothermal activity causing As to occur in arsenopyrite, silicates or carbonates, the shale, slate and phyllite sequence examined in the current study is likely applicable to aquifers in many areas underlain by variably metamorphosed bedrock.

In summary, the depletion of As, Cu, Ni, Pb and Zn in black pelitic rocks metamorphosed to temperatures greater than ~250–300 °C is due to low-grade metamorphism that leaches these relatively-mobile trace elements – especially those that reside in pyrite – out of the system. This has implications for bedrock aquifers situated in metasedimentary sequences; in particular, groundwater produced from black pelitic rocks exposed to temperatures <300 °C during metamorphism is more likely to have higher bulk rock As compared to correlative higher-grade rocks. Clearly, many biogeochemical and physical factors in addition to bulk rock geochemistry exert controls on As in groundwater, including microbial populations, composition of the groundwater itself (e.g. pH, Eh, carbonate species or other anions), and physical controls such as residence time. Nonetheless, the variance of bulk-rock As concentration as a function of low-grade metamorphism may prove to be a valuable variable in predicting and understanding groundwater composition in fractured bedrock aquifers.

## Acknowledgments

## References

Abraitis PK, Pattrick RAD, Vaughan DJ. Variations in the compositional, textural and electrical properties of natural pyrite: a review. Int J Miner Process 2004;74:41–59.

Anderson, C., 2006. Geochemistry of meta-sedimentary rocks in the Waterbury-Stowe area, central Vermont. Unpub. Bachelors Thesis, Middlebury College, Middlebury, Vermont. 65 pp.

Ayotte JD, Montgomery DL, Flanagan SF, Robinson KW. Arsenic in groundwater in eastern New England: occurrence, controls, and human health implications. Environ Sci Technol 2003;37:2075–83.

Ayotte JD, Bernard NT, Nuckols JR, Cantor KP, Robinson Jr GR, Baris D, et al. Modeling the probability of arsenic in groundwater in New England as a tool for exposure assessment. Environ Sci Technol 2006;40:3578–85.

Bebout GE, Ryan JG, Leeman WP, Bebout AE. Fractionation of trace elements by subduction-zone metamorphism effect of convergent-margin thermal evolution. Earth Planet Sci Lett 1999;171:63–81.

Birkeland PW. Soils and geomorphology. 3rd ed. New York: Oxford University Press; 1999.

Bock B, McLennan SM, Hanson GN. Geochemistry and provenance of the Middle Ordovician Austin Glen member (Normanskill formation) and the Taconian Orogeny in New England. Sedimentology 1998;45:635–55.

Brown LM, Zahm SH, Hoover RN, Fraumeni JF. High bladder cancer mortality in rural New England (United States): an etiologic study. Cancer Causes Control 1995;6:361–8.

Chan Y-C, Crespi JM, Hodges KV. Dating cleavage formation in slates and phyllites with the $^{40}$Ar/$^{39}$Ar laser microprobe: an example from the western New England Appalachians, USA. Terra Nova 2000;12:264–71.

Chesnaux R. Regional recharge assessment in the crystalline bedrock aquifer of the Kenogami Uplands, Canada. Hydrol Sci J 2013;58(2):1–16.

Cloutier V, Lefebvre R, Savard M, Bourque E, Therrien R. Hydrogeochemistry and groundwater origin of the Basses-Laurentides sedimentary rock aquifer system, St. Lawrence Lowlands, Québec, Canada. Hydrogeol J 2006;14:573–90.

DeSimone LA, Barbaro JR. Yield of bedrock wells in the Nashoba terrane, central and eastern Massachusetts: U.S. Geological survey scientific investigations report; 2012. p. 2012–5155 [74 pp. (Available at http://pubs.usgs.gov/sir/2012/5155)].

Garver JI, Royce PR, Smick TA. Chromium and nickel in shale of the Ordovician Taconic foreland: a case study for the provenance of sediments with an ultramafic provenance. J Sediment Res 1996;66:100–6.

Goldstein A, Selleck B, Valley JW. Pressure, temperature, and composition history of syntectonic fluids in a low-grade metamorphic terrane. Geology 2005;33:421–4.

Gromet LP, Dymek RF, Haskin LA, Korotev RL. The "North American shale composite"; its compilation, major and trace element characteristics. Geochim Cosmochim Acta 1984;48:2469–82.

Hattori K, Takahashi Y, Guillot S, Johanson B. Occurrence of arsenic (V) in forearc mantle serpentinites based on X-ray absorption spectroscopy study. Geochim Cosmochim Acta 2005;69:5585–96.

Hurowitz JA, McLennan SM. Geochemistry of Cambro-Ordovician sedimentary rocks of the Northeastern United States: changes in sediment sources at the onset of Taconian orogenesis. J Geol 2005;113:571–87.

Ibanez Y. Région Chaudière-Appalaches au Québec: les puits privés d'alimentation en eau potable sont-ils la principale source d'exposition chronique à l'arsenic? Mémoire EHESP d'Ingénieur du Génie Sanitaire. Sorbonne, Rennes, France: Ecole des Hautes Etudes en Santé Publique; 2008 [140 pp. Accessed on-line 30-December 2013: http://fulltext.bdsp.ehesp.fr/Ehesp/memoires/lgs/2008/ibanez.pdf].

Kennedy, G.W. and Finlayson-Bourque, D. 2011. Calcium in groundwater from bedrock aquifers in Nova Scotia. Nova Scotia Department of Natural Resources, Mineral Resources Branch, Open File Map ME 2011-018, scale 1: 500,000. Accessed on-line 13-Dec-2013: https://www.novascotia.ca/NATR/MEB/DATA/mg/ofm/pdf/ofm_2011-018_dp.pdf

Kolker A, Nordstrom DK. Occurrence and microdistribution of arsenic in pyrite. Proceedings of the USGS Arsenic Workshop. Denver: U.S. Geological Survey; 2001. [Accessed on-line 30-December 2013: http://wwwbrr.cr.usgs.gov/projects/GWC_chemtherm/FinalAbsPDF/kolker.pdf].

Kübler B. La cristallinité de l'illite et les zones tout à fait supérieures du métamorphisme. Etages Tectoniques, Colloque à Neuchâtel 1966. Neuchâtel, Suisse: A la Baconnière; 1967. p. 105–21.

Landing ED. Ediacaran–Ordovician of East Laurentia — geologic setting and controls on deposition along the New York Promontory region. In: Landing ED, editor. Ediacaran–Ordovician of East Laurentia: S.W. Ford Memorial Volume: New York State Museum Bulletin 510. Albany, New York: The University of the State of New York; 2007. p. 5–24.

Large R, Thomas H, Craw D, Henne A, Henderson S. Diagenetic pyrite as a source for metals in orogenic gold deposits, Otago schist, New Zealand. N Z J Geol Geophys 2012;55:137–49.

Lipfert G. A geochemical, isotopic, and petrologic study of a watershed with arsenic-enriched ground water in Northport, Maine [Ph.D. thesis] University of Maine; 2006.

Lipfert G, Reeve AC, Sidle WC, Marvinney R. Geochemical patterns of arsenic-enriched groundwater in fractured, crystalline bedrock, Northport, Maine, USA. Appl Geochem 2006;21:528–45.

Mango H. Source of arsenic in drinking water and groundwater flow pathways in southwestern Vermont. Geol Soc Am Abstr Programs 2009;41:8.

Novakowski KS, Lapcevic PA. Regional hydrogeology of the Silurian and Ordovician sedimentary rock underlying Niagara Falls, Ontario, Canada. J Hydrol 1988;104:211–36.

O'Shea B, Yang Q, MacLean A, Marvinney R, Brock P, Zheng Y. Arsenic in fractured bedrock aquifers: the influence of prograde metamorphism on arsenic mineralization in the bedrock. Geol Soc Am Abstr Programs 2008;40:473.

Peters SC. Arsenic in groundwaters in the Northern Appalachian Mountain belt: a review of patterns and processes. J Contam Hydrol 2008;99:8–21.

Peters SC, Burkert L. The occurrence and geochemistry of arsenic in groundwaters of the Newark Basin of Pennsylvania. Appl Geochem 2007;23:85–98.

Pitcairn IK, Olivo GR, Teagle DAH, Craw D. Sulfide evolution during prograde metamorphism of the Otago and Alpine schists. New Zealand. Can Mineral 2010;48:1267–95.

Ratcliffe, N.M., Stanley, R.S., Gale, M.H., Thompson, P.J., Walsh, G.J., 2011. Bedrock geologic map of Vermont: U.S. Geol. Survey Scientific Investigations Map 3184, 3 sheets, scale 1:100,000.

Reich M, Becker U. First-principles calculations of the thermodynamic mixing properties of arsenic incorporation into pyrite and marcasite. Chem Geol 2006;225:278–90.

Rowley DB, Kidd WSF. Stratigraphic relationships and detrital composition of the medial Ordovician flysch of western New England; implications for the tectonic evolution of the Taconic orogeny. J Geol 1981;89:199–218.

Ryan PC, Kim J, Wall AJ, Moen JC, Corenthal LG, Chow DR, et al. Ultramafic-derived arsenic in a fractured bedrock aquifer. Appl Geochem 2011;26:444–57.

Ryan PC, Kim J, Silverman A, Russell D. The effect of metamorphism on arsenic concentration in metapelite bedrock aquifers; a case study of the Connecticut Valley/Gaspe sequence (NE Vermont and SE Quebec). Geol Soc Am Abstr Programs 2012;44(7):52.

Ryan PC, Kim J, Mango H, Hattori K, Thompson A. Arsenic in a fractured slate aquifer system, New England (USA): influence of bedrock geochemistry, groundwater flow paths, redox and ion exchange. Appl Geochem 2013;39:181–92.

Scholz F, Neumann T. Trace element diagenesis in pyrite-rich sediments of the Achterwasser lagoon, SW Baltic Sea. Mar Chem 2007;107:516–32.

Schreiber ME, Gotkowitz MB, Simo JA, Freiberg OG. Mechanisms of arsenic release to ground water from naturally occurring sources, eastern Wisconsin. In: Welch AH, Stollenwerk KG, editors. Arsenic in ground water. Dordrecht: Kluwer Academic Publishers; 2003. p. 259–80.

Smedley PL, Kinniburgh DG. A review of the source, behavior and distribution of As in natural waters. Appl Geochem 2002;17:517–68.

Stanley RS, Ratcliffe NM. Tectonic synthesis of the Taconian orogeny in western New England. Geol Soc Am Bull 1985;96:1227–50.

Studwell SR. Arsenic concentrations within variably metamorphosed shales of the Taconic Sequence, Vermont and New York. Middlebury College, Middlebury, Vermont USA: Unpublished Bachelors Thesis; 2013. 51 pp.

Thompson, A.E., 2011, Geochemical and sulfur isotope analysis of taconic slates: implications for arsenic source and mobility in a bedrock aquifer system. Unpublished Bachelors Thesis, Middlebury College, Middlebury, Vermont USA. 70 pp.

Wang H, Frey M, Stern W. Diagenesis and metamorphism of clay minerals in the Helvetic Alps of eastern Switzerland. Clay Clay Miner 1996;44:96–112.

Warr LN, Rice AHN. Interlaboratory standardization and calibration of clay mineral crystallinity and crystallite size data. J Metamorph Geol 1994;12:141–52.

West Jr DP, Yates MG, Gerbi C, Barnard NQ. Metamorphosed Ordovician iron- and manganese-rich rocks in south-central Maine: from peri-Gondwanan deposition through Acadian metamorphism. Am Mineral 2008;93:270–83.

Yang Q, Jung HB, Marvinney RG, Culbertson CW, Zheng Y. Can arsenic occurrence rates in bedrock aquifers be predicted? Environ Sci Technol 2012;46:2080–7.

Zen E-A. Metamorphism of lower Paleozoic rocks in the vicinity of the Taconic Range in west-central Vermont. Am Mineral 1960;45:129–75.

Zen E-A. Some revisions in the interpretation of the Taconic allochthon in west-central Vermont. Geol Soc Am Bull 1972;83:2573–88.